Nucleic Acids Research Advance Access published May 31, 2009

Nucleic Acids Research, 2009, 1–7
doi:10.1093/nar/gkp442

The flexibility of locally melted DNA

Robert A. Forties[1], Ralf Bundschuh[1,2,3] and Michael G. Poirier[1,2,*]

[1]Department of Physics, [2]Department of Biochemistry and [3]Center for RNA Biology, The Ohio State University, 191 West Woodruff Avenue, Columbus, OH 43210-1117, USA

Received April 9, 2009; Revised May 8, 2009; Accepted May 11, 2009

ABSTRACT

Protein-bound duplex DNA is often bent or kinked. Yet, quantification of intrinsic DNA bending that might lead to such protein interactions remains enigmatic. DNA cyclization experiments have indicated that DNA may form sharp bends more easily than predicted by the established worm-like chain (WLC) model. One proposed explanation suggests that local melting of a few base pairs introduces flexible hinges. We have expanded this model to incorporate sequence and temperature dependence of the local melting, and tested it for three sequences at temperatures from 23°C to 42°C. We find that small melted bubbles are significantly more flexible than double-stranded DNA and can alter DNA flexibility at physiological temperatures. However, these bubbles are not flexible enough to explain the recently observed very sharp bends in DNA.

INTRODUCTION

Beyond the information content of a given DNA molecule, its physical properties as a polymer, such as its flexibility, are important for its biological function. The formation of sharp bends is critical to many biological processes such as gene regulation (1,2), binding of transcription factors (3,4) and DNA packaging (5). An accurate quantitative understanding of the formation of such bends is important.

The flexibility of a polymer is characterized by its persistence length, the length over which orientations of the polymer become decorrelated. For DNA on scales longer than several hundred base pairs this flexibility has been investigated using many methods, including cyclization (6–8), direct mechanical measurements of force versus extension (9,10), and atomic force microscopy (AFM) (11,12). Data from these experiments all fit the worm-like chain (WLC) model, which treats DNA as a uniform rod with a given bending rigidity (13). The numerical values of the persistence length recovered in these experiments are in the range of 40 to 55 nm.

Recent studies suggest that the WLC may not accurately describe sharp bends in DNA (14–18). For example, cyclization experiments for the biologically important regime of sequence lengths below 200 bp indicate that sharp bends occur significantly more frequently than predicted by the WLC model (14,15). While the results of these studies were recently challenged (8), the large sequence dependence in the flexibility reported remains unchallenged. Furthermore, fluorescence resonance electron transfer (FRET) measurements (16,17) and AFM studies (18) also indicate that on short length scales DNA is more flexible than predicted by the WLC model. Together, these studies suggest that a modification of the WLC model appears necessary to explain sequence-dependent sharp bends in DNA.

One explanation of the increased flexibility of double-stranded DNA (dsDNA) on short length scales is that DNA may transition to kinked structures, which maintain base pairing (19,20). This notion is supported by recent investigations of DNA minicircles (21) and with AFM measurements, which show that the DNA bending energy is not harmonic for all deflections (18,22). An alternative but not mutually exclusive model for the measured flexibility of short DNA molecules is the formation of melted bubbles in DNA, where a number of contiguous nucleotides are unpaired. These bubbles may form spontaneously as thermal excitations. Indeed, Yan and Marko (23,24) suggest that cyclization of short DNA sequences may be explained if small bubbles are significantly more flexible than dsDNA, since for short molecules the gain in bending energy due to a flexible hinge can outweigh the loss in free energy of breaking the DNA base pairing. In order to judge the relevance of this mechanism for the anomalous flexibility of short DNA molecules, the gain in bending energy and the loss of base pairing free energy must be quantified. The latter has been measured experimentally in a temperature- and sequence-dependent manner (1,25,26). Thus, to accurately predict the flexibility of the molecule with this model, measurements of the effective flexibility of melted bubbles are required.

Here, we report measurement of the flexibility of small melted bubbles. We perform cyclization experiments for three different sequences at temperatures from 23°C to 42°C, and then fit the bubble flexibilities needed such

*To whom correspondence should be addressed. Tel: +1 614 247 4493; Fax: +1 614 292 7557; Email: mpoirier@mps.ohio-state.edu

that a sequence-dependent Yan–Marko model makes predictions that agree with our cyclization data. We find that small bubbles have modest persistence lengths, of 8 and 4 nm for 3- and 4-bp bubbles, respectively. We report persistence lengths at a reference temperature of 294 K. The persistence length decreases with temperature, so we must scale its value when comparing with experiments at different temperatures (Supplementary Data). This is consistent with the expectation that small bubbles should be significantly more flexible than dsDNA (16,23) and is also consistent with measurements on DNA containing mismatches of similar length (16,27,28). Our results imply that melted bubbles are important to DNA flexibility, but that other effects such as kinking (19,20) are also needed to explain the very sharp bends observed in some AFM experiments (18) and in DNA minicircles (21).

MATERIALS AND METHODS

We develop a model that predicts the impact of melted bubbles on the overall flexibility of dsDNA. We then make temperature-dependent cyclization measurements on a 200-bp fragment of DNA from bacteriophage λ, which has previously been studied at room temperature (7). This allows us to make a rough estimate of the flexibilities for small melted bubbles, which we use to design a pair of DNA fragments with nearly identical sequences which our model predicts should have significantly different flexibilities. We then perform temperature-dependent cyclization measurements (6) for these sequences to test the predictions of our model.

Model and theory

We describe the flexibility of dsDNA using a WLC model reduced to discrete units (discretized) following the work of Yan *et al.* (24). In this model, the bending free energy of a discretized polymer of N segments is

$$E_{WLC} = \sum_{n=1}^{N-1} \frac{A}{2b}\theta_n^2 \times k_B T. \quad \mathbf{1}$$

Here A is the persistence length, b is the segment length, θ_n is the angle between two adjacent segments of the polymer, k_B is Boltzmann's constant and T is temperature.

We apply this model to dsDNA with a segment length of 1 nt, or $b = 0.34$ nm. In our calculations, we use $A = A_{ds}$ between 40 and 55 nm, which is within the range of dsDNA persistence lengths reported in the literature (6–9,11,13). We then include the formation of melted bubbles. These are structures where a stretch of bases becomes unpaired resulting in a higher flexibility than base paired dsDNA (23,24). The associated melting free energy for a bubble containing L open base pairs starting at base α is $\mu_{\alpha L} = \sum_{i=\alpha}^{\alpha+L} \mu_i^{st} + \mu_{\alpha L}^{loop}$, where μ_i^{st} is the free energy cost to break the stacking interaction between base pairs i and $i-1$, and $\mu_{\alpha L}^{loop}$ is the entropic contribution that arises from the formation of a closed loop in a flexible polymer, called the loop entropy (26) or ring factor (29). The free energy to break the hydrogen bonding between base pairs is included in the stacking interaction, such that if a single base pair i is broken, $\mu_i^{st} + \mu_{i+1}^{st}$ will give the total free energy cost of breaking the hydrogen bonds in base pair i and the stacking interactions between base pairs from $i-1$ to i, and from i to $i+1$. Sequence-dependent values have been explicitly measured for μ_i^{st} (1,25,26), and $\mu_{\alpha L}^{loop}$ for $L \leq 2$ (26). The exact values of stacking energies and loop entropies for DNA used in this study have not been published, but are available upon request from David Mathews. The analogous values for RNA along with a description of how Mathews *et al.* obtained these values may be found in (26). For larger values of L, we use $\mu_{\alpha L}^{loop} = \mu_L^{avg} + \mu_\alpha^d + \mu_{\alpha+L}^d$, where μ_L^{avg} is the average loop entropy of a size L bubble, and μ_α^d is a correction to this which depends on the last stacking interaction broken at each edge of the bubble. All needed values of μ_α^d and μ_L^{avg} have been measured (26). All these free energies have been determined in melting experiments and thus include an entropic contribution from the configurational degrees of freedom. Since we model the spatial configurations explicitly, we remove the configurational contributions from these measured free energy parameters (19, Supplementary Data). We model bubbles whose flexibility is isotropic about the helical axis of the DNA. The free energy for a bubble is

$$E_{Bubble} = \mu_{\alpha L} + \sum_{n=\alpha}^{\alpha+L-1} \frac{A_L}{2b_L}\theta_n^2 \times k_B T, \quad \mathbf{2}$$

where A_L is the persistence length for a segment containing L open base pairs, and b_L is the segment length for an unpaired nucleotide, which we set equal to 0.7 nm, the segment length of single-stranded DNA (ssDNA). If a different value of b_L was used, we would need to adjust our values for A_L proportional to the change in b_L to give the same fit to our data. The total bending free energy E for a configuration is calculated using Equation (1) for all closed base pairs and Equation (2) for base pairs inside melted bubbles.

In order to be cyclized, a DNA molecule must form a closed loop whose ends meet with a parallel orientation. In principle, the DNA molecule may explore many states due to thermal fluctuations most of which do not lead to closed loops. In order to quantitatively compare with the cyclization experiments, we calculate the probability of loop closure, also called the J factor, as the total probability of all the DNA configurations that lead to a closed loop with parallel ends. For details of the calculation of this probability, see the Supplementary Data and (24).

The only free variables in our model are the persistence lengths of duplex DNA A_{ds}, and of internal bubbles A_L. We restrict the persistence length of duplex DNA to the reported values of 40–55 nm (6–9,11,13). We fit the J factor at 23°C by varying the duplex DNA persistence length. Variations in the J factor at this temperature are likely due to sequence-dependent intrinsic bend and twist (20,30,31). Once the duplex persistence length is determined for the DNA sequence, we compare the predictions of our model with experimentally measured J factors, and vary A_L to simultaneously give the best agreement at 30, 37 and 42°C. While we must use different A_{ds} for the

Figure 1. Synthetic 116-bp DNA sequences. The sequences are identical except for 8 nucleotides, which are highlighted with bold text and underlined. Both sequences have Cy5 fluorophores attached to thymine residues where shown.

different sequences, we fit all three sequences at all temperatures using a single set of A_L.

Cyclization experiments

We begin by measuring a 200-bp λ DNA sequence that has already been well studied (7,14). The 200-bp λ sequence is polymerase chain reaction (PCR) amplified from λ DNA, and then inserted into the pDrive plasmid (Qiagen). In addition, we study two synthetic 116-bp sequences, shown in Figure 1, which we design to have significantly different J factors using our model. The 116-bp sequences are synthesized by PCR amplification of custom DNA oligonucleotides (Operon). They are then digested with HindIII restriction endonuclease (20 U/μl; NEB) and inserted into the HindIII site of the pUC19 plasmid. All plasmid sequences are verified using a 3730 DNA Analyzer (Applied Biosystems).

In all cases, plasmids are replicated in DH5α *Escherichia coli* and harvested with a QIAprep Spin Miniprep kit (Qiagen). Custom oligonucleotides containing Amino Modifier C6 dT (Operon) are labeled at the modified residues with Cy5 fluorophores (Amersham) and purified using a C18 reverse phase high performance liquid chromatography (HPLC) column (Vidac). These oligonucleotides are then used to PCR amplify inserted sequences from plasmids, resulting in one Cy5 label per DNA molecule. Labeling DNA with Cy5 via an amino-modifier C6 dT is unlikely to impact the structure of the DNA because it is attached to the carbon 5 of a thymine base with a long hydrocarbon linker. To confirm this, we verify that our measurements of the 200-bp λ sequence labeled with Cy5 give the same result as those in (7), which were obtained with radiolabeled DNA. The labeled DNA is digested with HindIII leaving AGCT overlapping ends, and then purified using a Gen-Pak Fax ion exchange HPLC column (Waters). We ligate with an excess of ligase to verify that ligatability of the digested ends is $>95\%$.

Cyclization experiments are performed using T4 DNA ligase (400 U/μl; NEB) in its standard buffer, with 0.1 mg/ml bovine serum albumin (BSA) (10 mg/ml; NEB) added. Cy5 labeled, HindIII-digested DNA is added at a concentration of 0.33 nM for 116-bp sequences and 10 nM for the 200-bp sequence. T4 ligase is added in concentrations of 25–100 U/ml, over a range of temperatures from 23°C to 42°C. Ligation is found to be linear for ligase

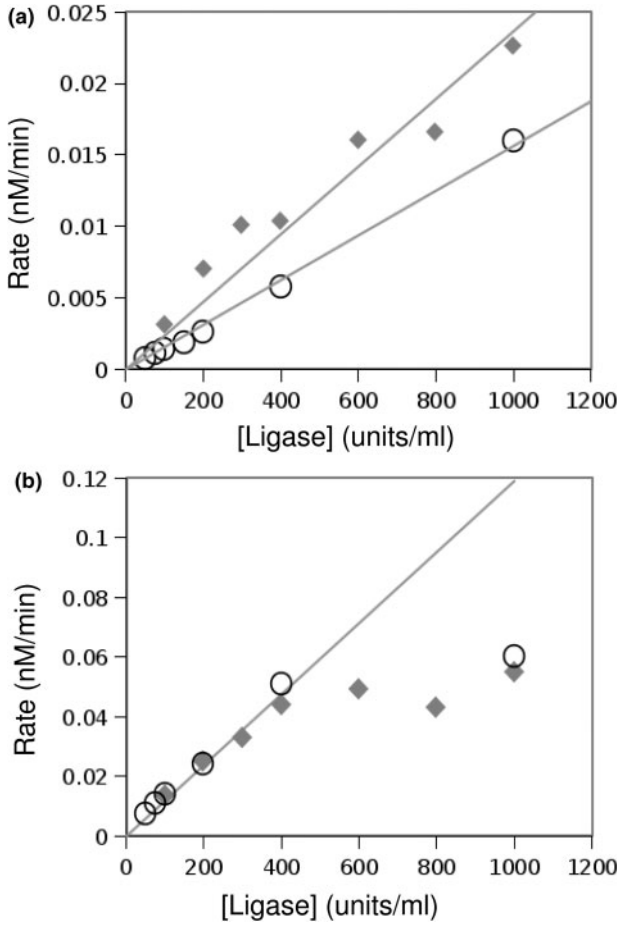

Figure 2. Rate of ligation versus concentration of T4 ligase at 37°C. The open circles show data from the 116o sequence, and the closed diamonds show data from the 116cl sequence. (**a**) The rate of formation of circular monomer increases linearly for all concentrations of ligase. (**b**) At high ligase concentration, the rate of dimer formation no longer increases linearly with ligase concentration. We find that ligation is linear up to 400 U/ml of ligase at 37°C, and therefore use ≤100 U/ml for our experiments at this temperature.

concentrations <100 U/ml at 23°C, in agreement with previous studies (8). Figure 2 shows that we also find that ligation is linear for ligase concentrations up to 400 U/ml at 37°C. Ligase activity is quenched by increasing the ethylenediaminetetraacetic acid (EDTA) concentration to 0.05 M and samples are digested with proteinase K (Invitrogen) for 20 min at 65°C to inactivate ligase. We repeat experiments at several T4 ligase concentrations to ensure reproducibility. For the 116-bp sequences samples are concentrated by precipitation with linear polyacrylamide (32). Samples are visualized on 6% polyacrylamide gels. The gels are then imaged using a Typhoon Trio imager (GE Healthcare) set to detect the Cy5-labeled DNA in order to determine the concentration of the different ligation products.

The J factor is calculated from cyclization experiments using (6):

$$J = 2M_0 \lim_{t\to 0} C(t)/D(t), \qquad \textbf{3}$$

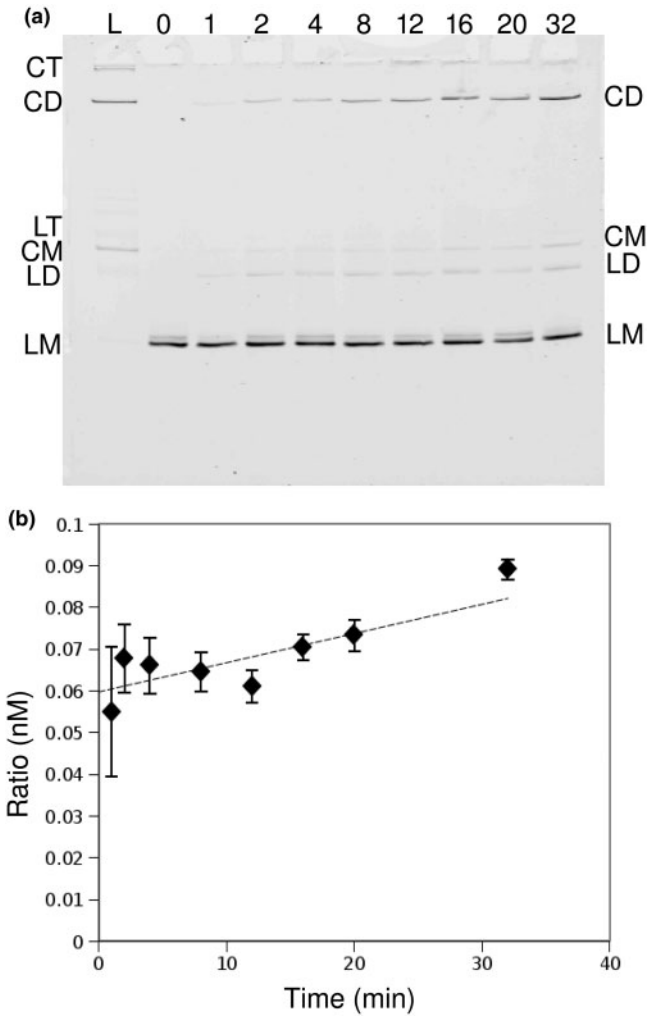

Figure 3. Example gel showing a ligation time course for the 116o sequence at a concentration of 0.33 nM ligated at 37°C with 50 U/ml T4 ligase. (**a**) Gel image showing both linearly and circularly ligated products. The bands in the gel are (from bottom to top) linear monomer (LM), linear dimer (LD), circular monomer (CM), linear trimer (LT), circular dimer (CD) and circular trimer (CT). The leftmost lane (labeled L) shows ligation with excess ligase, where almost all DNA is converted to circular products showing that it is at least 95% ligatable. The remaining lanes show a ligation time course, and are labeled with the reaction time in minutes. (**b**) A plot of the ratio $2M_0C(t)/D(t)$ created from the gel shown in (a). The intercept of this plot at $t = 0$ gives the J factor measured in this experiment. The LM band shows some sample impurity, which we measured to be <5%.

where M_0 is the initial concentration of the linear monomer of our DNA molecule, $C(t)$ is the concentration of cyclized monomer, which is one molecule ligated to itself forming a closed loop and $D(t)$ is the combined concentration of linear dimers and dimer circles, which may form directly from linear dimers. Since the only difference between the reactions that generate circular monomer and linear dimer is that for the former case, the DNA must bend into a closed loop while in the latter case it does not, the J factor gives a direct measure of DNA flexibility. Figure 3 shows an example of how the J factor is calculated from our experiments.

RESULTS

The results of cyclization experiments plotted alongside our sequence-dependent Yan–Marko model predictions for the three DNA molecules are shown in Figure 4. Also shown is the result of Vologodskaia and Vologodskii (7) for the 200 bp λ sequence, which quantitatively agrees with our measurements at 23°C. We adjusted the dsDNA persistence lengths of the 200 bp λ, 116cl and 116o molecules to 51, 44 and 48 nm, respectively, to fit the measured J factors at 23°C. These persistence length values are within the range reported in the literature (6–9,11,13). At 23°C, the excitations of melted base pairs are so rare that they do not contribute significantly to the J factor (Figure 4). These variations in J factors are likely to be due to other effects such as sequence-dependent permanent bend, twist and anisotropic bending and twisting fluctuations (19,20,30,31,33). We also note that TA stacks (a T followed by an A in the DNA sequence) periodic with the helical repeat have been suggested to promote cyclization (14,15), and that the 116o sequence contains eight TA stacks not found in the 116cl sequence. We therefore placed these TA stacks such that no pair is separated by an integer number of helical repeats to minimize any contribution to cyclization from this effect. It is possible that if this effect is due to permanent bendedness of TA stacks, such out of phase bends could be partially responsible for the 116o sequence having a smaller J factor than the 116cl sequence at 23°C.

The measurements of Du *et al*. (8) show that 116-bp sequences should have nearly an integer number of helical repeats, and therefore be relaxed with respect to twist when they are cyclized. However, the difference in J factor between 116o and 116cl at 23°C suggests that 116o might have a different helical repeat, and therefore might not be relaxed when cyclized. This would make interpretation of our results more difficult as we would have to consider the impact of twist on the J factor. Therefore, we measure the cyclization of a 116o sequence truncated to 114 bp and one extended to 118 bp. We find little variation of the J factor with length, indicating that the 116o sequence can be no more than 2 bp from an integer helical repeat. Since the integer helical repeat corresponds to a maximum in the twist dependence of the J factor, in the vicinity of such a maximum twist effects on the J factor are minimal and we are thus justified to neglect the effects of twist in our analysis (Supplementary Data).

While the J factors for 200 bp λ and 116cl may be fit at all temperatures by the WLC model, as indicated by the dashed lines in Figure 4, the 116o molecule cannot. It has a 5-fold increase in the J factor as compared with the WLC model at 37°C. This increase in J factor appears too large to be explained by known temperature-dependent structural changes in DNA, such as changes in the helical repeat (34). Since 116o forms melted bubbles more readily than the other sequences, this suggests that bubbles may impact the flexibility of short dsDNA molecules at 37°C.

Bubble flexibility

The effect of local melting on DNA flexibility depends on the frequency with which local melting occurs, which

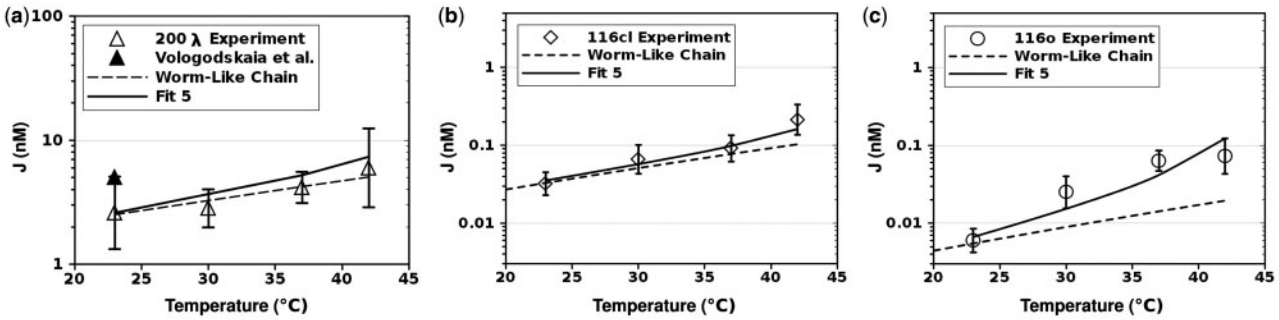

Figure 4. Measured *J* factors as a function of temperature. In all plots, the predictions of the WLC are shown by the dashed line, and the predictions of the sequence-dependent Yan–Marko model for Fit 5 are shown by the solid line. Fits 1–4 are nearly indistinguishable from Fit 5, and are shown as Supplementary Data. (**a**) A 200-bp fragment of λ DNA, with our experimental data shown by the open triangles and data from (7) shown by the closed triangle. (**b**) The 116cl sequence (open diamonds) is a 116-bp sequence designed to minimize the formation of local bubbles, while (**c**) the 116o sequence (open circles) is designed to readily form local bubbles in several locations.

we calculate based on known parameters, and on the (unknown) flexibility of those melted regions. Thus, by using our sequence-dependent Yan–Marko model to simultaneously fit our *J* factor measurements for all three DNA molecules with a single set of persistence lengths, we can constrain the range of persistence lengths for different size bubbles. Clearly, the bubbles cannot be more stiff than dsDNA and cannot be less stiff than two parallel ssDNA molecules, i.e. 2 nm (35). We also assume that the persistence length cannot increase as the bubble size increases. Furthermore, we find that we need only consider bubbles containing $\leq$4 bp, as larger bubbles occur so infrequently due to their large free energy cost that they cannot affect our model predictions.

We will now describe a series of fits where we constrain a subset of the bubble persistence lengths to be equal, and set the remaining bubble persistence lengths to a fixed extreme value (either equal to the persistence length of dsDNA or ssDNA). This leaves us with one adjustable parameter, which we manually vary to give the best overall fit to our data. We first fit the temperature dependence of all three DNA molecules with a constant persistence length for all melted bubbles. The observations provide a fit value of 13 nm as a 'lower limit' for the persistence length of 1-bp bubbles. To determine the 'maximum' persistence length for 1-bp bubbles, we determine how stiff we can make the 1-bp bubbles by reducing the persistence length of $\geq$2-bp bubbles. We find that 1-bp bubbles can have persistence length equal to dsDNA if $\geq$2-bp bubbles have a persistence length of 7 nm. This provides an 'upper limit' of dsDNA persistence length for 1-bp bubbles and a 'lower limit' for 2-bp bubbles of 7 nm. We then fit the data where 1- and 2-bp bubbles are as stiff as dsDNA and find that 3- and 4-bp bubbles must have a persistence length of 6 nm. This implies that 2-bp bubbles have a 'maximum' persistence length equal to that of dsDNA and that 3-bp bubbles have a 'minimum' persistence length of 6 nm. We finally attempt to fit the cyclization data assuming 1-, 2- and 3-bp bubbles are as stiff as dsDNA. However, we find no fit is possible even with a persistence length for 4-bp bubbles equal to that of two parallel ssDNA molecules, 2 nm, unless we also include 3-bp bubbles with a persistence length of at most 11 nm.

Table 1. Persistence lengths used to fit our data, given in nanometers at a reference temperature of 294 K

Bubble size	Fit 1	Fit 2	Fit 3	Fit 4	Fit 5	Range
1 bp	13	DS	DS	DS	32	13 to DS
2 bp	13	7	DS	DS	16	7 to DS
3 bp	13	7	6	11	8	6–13
4 bp	13	7	6	2	4	2–13

An entry of 'DS' indicates a persistence length equal to that of dsDNA, which is 44, 48 and 51 nm for 116cl, 116o and the 200 bp λ fragment, respectively. The five 'Fit' columns show values used in different fits to our data. The column labeled 'Range' summarizes the minimum and maximum persistence lengths that may be used to fit our data for each bubble size, found by inspecting fits 1–4.

The ranges of persistence lengths for different bubble sizes are summarized in Table 1. Plots of all fits compared with our experimental measurements are shown in the Supplementary Data. We view Fits 1–4 as unlikely because we expect a smooth decrease in persistence length as the bubble size increases, which converges to the single strand persistence length limit at 4–5 bp. To obtain a more realistic fit we first assume that 3-bp bubbles have a persistence length of 8 nm, which is that measured for 3-bp mismatches (28). We then arbitrarily choose a geometric scaling to provide a simple, smooth dependence. A scale factor of 2 results in the parameters shown in Table 1, Fit 5, which give a good fit to our data as shown in Figure 4. While there is a very large possible range of persistence lengths for 1 and 2 bp bubbles which fit our data, we view the values given by Fit 5 as the most physically reasonable approximate values for all persistence lengths.

Melted bubbles $>$4 bp do not occur often enough to contribute to the cyclization of DNA, but we may still infer their flexibility indirectly from our experiments. We find that 4-bp bubbles display persistence length not much higher than that of two ssDNA molecules. Bubbles $>$4 bp can neither display persistence length larger than the persistence length of 4-bp bubbles nor be less stiff than two ssDNA molecules. Therefore, we conclude that bubbles

>4 bp have essentially the same persistence length as that of two ssDNA molecules.

DISCUSSION

We provide a model that can accurately predict the impact of melted bubbles on DNA flexibility. To demonstrate the viability of this model, we perform cyclization measurements for nearly identical sequences, which our model predicts should have significantly different *J* factors. The results of these experiments are in agreement with the predictions of our model. The WLC model also correctly predicts *J* factors for the 200 bp λ and 116cl sequences, but not the 116o sequence, which we predict should readily form melted bubbles. Our model simultaneously predicts the behavior of all three sequences with a single set of persistence lengths for melted bubbles, indicating that the formation of melted bubbles may in fact explain the differences we measure between the 116o and 116cl sequences.

By comparing our model to experimentally determined *J* factors at different temperatures, we constrain the persistence lengths of 3- and 4-bp bubbles to the ranges of 6–13 and 2–13 nm, respectively. We estimate that 1-, 2-, 3- and 4-bp bubbles have persistence lengths of roughly 32, 16, 8 and 4 nm, respectively. We also find that bubbles >4 bp have a persistence lengths equal to that of two ssDNA molecules, or ~2 nm (35).

Our fit values for the persistence length of 3 bp melted bubbles are in very good agreement with measurements of the flexibility of three consecutive mismatches (28). This implies that mismatches may have similar physical properties to thermally excited melted bubbles, and that our values for persistence lengths of melted bubbles may be good estimates of mismatch flexibilities (36).

The bubble persistence lengths we find also suggest that the main impact of melted bubbles on DNA bending comes from those in the 2- to 4-bp range, and especially 3-bp bubbles. Larger bubbles occur too infrequently to make a significant impact on bending, while the large persistence length of 1-bp bubbles causes them to contribute very little to overall flexibility. Therefore, a model such as ours with isotropic bending cannot explain experiments which measure large flexibilities for 1-bp mismatches (16,27). This would instead require a model including kinks or directional bends (19,20).

There is currently a discrepancy between reported measurements of the *J* factor for DNA molecules significantly less than the DNA persistence length (~150 bp) (8,14,15). While our results cannot fully explain these discrepancies, we can make some conclusions that impact this issue. First, we measure *J* factors for our sequences that agree with Du *et al.* (8). Therefore, certain 116-bp DNA sequences have *J* factors that are similar to those predicted by the WLC model. Second, we find that the *J* factor for our 116o sequence increases by 4-fold between 23°C and 30°C. Du *et al.* performed their measurements at 21°C, while Cloutier *et al.* made theirs at 30°C, so it is possible that the temperature difference could be partially responsible for their different results. Third, we measure a 4-fold difference in *J* factors between our nearly identical 116-bp sequences at 23°C, which cannot be explained by our model and indicates that different sequences could have very different *J* factors. Du *et al.* and Cloutier *et al.* measured *J* factors for different sequences. In fact, some of the sequences studied by Cloutier *et al.* were selected to preferentially wrap into nucleosomes (37). These variations in the DNA sequences could explain some of the differences between these studies.

Our results demonstrate that sequence-dependent dsDNA melting can increase the flexibility of dsDNA such that the *J* factor is increased to 5-fold more than predicted by the WLC model at 37°C. We show that such a large increase in *J* factor cannot be due to a decrease in twist rigidity with temperature, reinforcing our assertion that this effect is due to the formation of melted bubbles. However, this increase in the *J* factor is of the same order of magnitude as differences we observe between sequences at lower temperatures, where DNA melting does not contribute to increasing the *J* factor. Moreover, we verified that DNA melting alone using the bubble flexibilities determined in our experiments cannot explain the sharp bends recently observed in AFM studies (18) and FRET experiments (16,17) (Note that the FRET experiments (16,17) were performed under significantly different salt conditions from cyclization experiments that make only qualitative but not quantitative comparisons between these and our experiments meaningful). We conclude that an accurate model of DNA flexibility at physiological temperatures must include both melted bubbles and other effects such as sequence-dependent bends and twists (19,20,30,31,33).

SUPPLEMENTARY DATA

Supplementary Data are available at NAR Online.

ACKNOWLEDGEMENTS

We thank A. Vologodskii for allowing us to reproduce results from (7); K. Musier-Forsyth for access to a Typhoon Trio gel scanner; and R. Fishel for helpful discussions of this work.

FUNDING

National Science Foundation Graduate Research Fellowship (to R.A.F.); Career Award in the Basic Biomedical Sciences from the Burroughs Wellcome Fund and the National Institutes of Health (R01 GM083055 to M.G.P.) Petroleum Research Fund of the American Chemical Society (42555-G9) and the National Science Foundation (DMR-0706002 to R.B.). Funding for open access charge: National Institutes of Health (R01 GM083055).

Conflict of interest statement. None declared.

REFERENCES

1. Adhya,S. (1989) Multipartite genetic control elements – communication by DNA loop. *Annu. Rev. Genet*., **23**, 227–250.
2. Moslaluk,C. and Bastia,D. (1987) DNA bending is induced in an enhancer by the DNA-binding domain of the bovine papillomavirus E2 protein. *Proc. Natl Acad. Sci. USA*, **85**, 1826–1830.
3. Horikoshi,M., Bertuccioli,C., Takada,R., Wang,J., Yamamoto,T. and Roeder,R.G. (1992) Transcription factor TFIID induces DNA bending upon binding to the TATA element. *Proc. Natl Acad. Sci. USA*, **89**, 1060–1064.
4. Rees,W., Keller,R., Vesenka,J., Yang,G. and Bustamante,C. (1987) Evidence of DNA bending in transcription complexes imaged by scanning force microscopy. *Science*, **260**, 1646–1649.
5. Nelson,D.L. and Cox,M.M. (2005) In Freeman,W.H. (ed.), *Principles of Biochemistry*, New York.
6. Shore,D. and Baldwin,R.L. (1983) Energetics of DNA twisting. *J. Mol. Biol*., **170**, 957–981.
7. Vologodskaia,M. and Vologodskii,A. (2002) Contribution of the intrinsic curvature to measured DNA persistence length. *J. Mol. Biol*., **317**, 205–213.
8. Du,Q., Smith,C., Shiffeldrim,N., Vologodskaia,M. and Vologodskii,A. (2005) Cyclization of short DNA fragments and bending fluctuations of the double helix. *Proc. Natl Acad. Sci. USA*, **102**, 5397–5402.
9. Bustamante,C., Marko,J.F., Siggia,E.D. and Smith,S. (1994) Entropic elasticity of lambda-phage DNA. *Science*, **265**, 1599–1600.
10. Wang,M.D., Yin,H., Landick,R., Gelles,J. and Block,S.M. (1997) Stretching DNA with optical tweezers. *Biophys. J*., **72**, 1335–1346.
11. Hansma,H.G., Revenko,I., Kim,K. and Laney,D.E. (1996) Atomic force microscopy of long and short double-stranded, single-stranded and triple-stranded nucleic acids. *Nucleic Acids Res*., **24**, 713–720.
12. Hansma,H.G., Kim,K.J., Laney,D.E., Garcia,R.A., Argaman,M., Allen,M.H. and Parsons,S.M. (1997) Properties of biomolecules measured from atomic force microscope images: a review. *J. Struct. Biol*., **119**, 99–108.
13. Hagerman,P.J. (1988) Flexibility of DNA. *Annu. Rev. Biophys. Biophys. Chem*., **17**, 265–286.
14. Cloutier,T.E. and Widom,J. (2004) Spontaneous sharp bending of double-stranded DNA. *Mol. Cell*, **14**, 355.
15. Cloutier,T.E. and Widom,J. (2005) DNA twisting flexibility and the formation of sharply looped protein-DNA complexes. *Proc. Natl Acad. Sci. USA*, **102**, 3645–3650.
16. Yuan,C.L., Chen,H.M., Lou,X.W. and Archer,L.A. (2008) DNA bending stiffness on small length scales. *Phys. Rev. Lett*., **100**, 18102.
17. Shroff,H., Sivak,D., Siegel,J.J., McEvoy,A.L., Siu,M., Spakowitz,A., Geissler,P.L. and Liphardt,J. (2008) Optical measurement of mechanical forces inside short DNA loops. *Biophys. J*., **94**, 2179–2186.
18. Wiggins,P.A., Van der Heijden,T., Moreno-Herrero,F., Spakowitz,A., Phillips,R., Widom,J., Dekker,C. and Nelson,P.C. (2006) High flexibility of DNA on short length scales probed by atomic force microscopy. *Nat. Nanotechnol*., **1**, 137–141.
19. Chen,H., Liu,Y., Zhou,Z., Hu,L., Ou-Yang,Z. and Yan,J. (2009) Temperature dependence of circular DNA topological states. *Phys. Rev. E*, **79**, 41926.
20. Chen,H. and Yan,J. (2008) Effects of kink and flexible hinge defects on mechanical responses of short double-stranded DNA molecules. *Phys. Rev. E*, **77**, 41907.
21. Du,Q., Kotlyar,A. and Vologodskii,A. (2008) Kinking the double helix by bending deformation. *Nucleic Acids Res*., **36**, 1120–1128.
22. Wiggins,P.A. and Nelson,P.C. (2006) Generalized theory of semi-flexible polymers. *Phys. Rev. E*, **73**, 31906.
23. Yan,J. and Marko,J.F. (2004) Localized single-stranded bubble mechanism for cyclization of short double helix DNA. *Phys. Rev. Lett*., **93**, 108108.
24. Yan,J., Kawamura,R. and Marko,J.F. (2005) Statistics of loop formation along double helix DNAs. *Phys. Rev. E*, **71**, 61905.
25. SantaLucia,J. (1998) A unified view of polymer, dumbbell, and oligonucleotide DNA nearest-neighbor thermodynamics. *Proc. Natl Acad. Sci. USA*, **95**, 1460–1465.
26. Mathews,D.H., Disney,M.D., Childs,J.L., Schroeder,S.J., Zuker,M. and Turner,D.H. (2004) Incorporating chemical modification constraints into a dynamic programming algorithm for prediction of RNA secondary structure. *Proc. Natl Acad. Sci. USA*, **101**, 7287–7292.
27. Isaacs,R.J. and Spielmann,H.P. (2004) Insight into G-T mismatch recognition using molecular dynamics with time-averaged restraints derived from NMR spectroscopy. *J. Am. Chem. Soc*., **126**, 583–590.
28. Kahn,J.D., Yun,E. and Crothers,D.M. (1994) Detection of localized DNA flexibility. *Nature*, **368**, 163–166.
29. Krueger,A., Protozanova,E. and Frank-Kamenetskii,M.D. (2006) Sequence-dependent basepair opening in DNA double helix. *Biophys. J*., **90**, 3091–3099.
30. Coleman,B.D., Olson,W.K. and Swigon,D. (2003) Theory of sequence-dependent DNA elasticity. *J. Chem. Phys*, **118**, 7127–7140.
31. Becker,N.B., Wolff,L. and Everaers,R. (2006) Indirect readout: detection of optimized subsequences and calculation of relative binding affinities using different DNA elastic potentials. *Nucleic Acids Res*., **34**, 5638–5649.
32. Gaillard,C. and Strauss,F. (1990) Ethanol precipitation of DNA with linear polyacrylamide as carrier. *Nucleic Acids Res*., **18**, 378.
33. Rouzina,I. and Bloomfield,V.A. (1998) DNA bending by small, mobile multivalent cations. *Biophys. J*., **74**, 3152–3164.
34. Duguet,M. (1993) The helical repeat of DNA at high temperature. *Nucleic Acids Res*., **21**, 463–468.
35. Achter,E.K. and Felsenfeld,G. (1971) ssDNA persistence length. *Biopolymers*, **10**, 1625–1634.
36. Mazurek,A., Johnson,C.N., Germann,M.W. and Fishel,R. (2009) Sequence context effect for hMSH2-hMSH6 mismatch-dependent activation. *Proc. Natl Acad. Sci. USA*, **106**, 4177–4182.
37. Lowary,P.T. and Widom,J. (1998) New DNA sequence rules for high affinity binding to histone octamer and sequence-directed nucleosome positioning. *J. Mol. Biol*., **276**, 19–42.